Distribution of neurones expressing inwardly rectifying and Ca^{2+}-permeable AMPA receptors in rat hippocampal slices

Tadashi Isa, Shun-ichi Itazawa, Masae Iino, Keisuke Tsuzuki and Seiji Ozawa*

Department of Physiology, School of Medicine, Gunma University, 3-39-22 Showa-machi, Maebashi, Gunma, Japan, 371

1. Current–voltage (I–V) relationships and Ca^{2+} permeability of receptor channels activated by bath application of kainate, a non-desensitizing agonist of α-amino-3-hydroxy-5-methyl-4-isoxazolepropionic acid (AMPA) receptors, were examined in various types of neurones in hippocampal slices of 5- to 13-day-old rats by using the tight-seal patch clamp recording technique.

2. Three types of responses were observed: type I response with outwardly rectifying I–V relationship, type II response with I–V relationship of marked inward rectification, and intermediate response with I–V relationship of weaker inward rectification. Neurones with type I, type II and intermediate I–V relationships of kainate responses were referred to as type I, type II and intermediate neurones, respectively.

3. Permeability of Ca^{2+} ions was estimated by the reversal potential of kainate response in the outside-out patch in Na^+-free extracellular solution containing 100 mM Ca^{2+}. The reversal potentials were $-44{\cdot}4 \pm 14{\cdot}0$ mV (mean ± S.D.) for type I ($n = 7$), $+11{\cdot}8 \pm 3{\cdot}6$ mV for type II ($n = 5$), and $-8{\cdot}7 \pm 7{\cdot}4$ mV for the intermediate neurones ($n = 7$). The values of P_{Ca}/P_{Cs}, the ratios of the permeability coefficients of Ca^{2+} and Cs^+, estimated according to the constant-field equation were 0·08 for type I, 1·71 for type II, and 0·50 for the intermediate neurones.

4. Type II and intermediate responses were observed mainly in non-pyramidal neurones in various areas of the hippocampus, most frequently observed in the stratum moleculare of the dentate gyrus and in the stratum radiatum and the stratum lacunosum-moleculare of both the CA1 and CA3 regions. Both type II and intermediate neurones stained with biocytin had round- or ellipsoidal-shaped somata and issued divergent axonal projections to the surrounding structures.

5. Excitatory postsynaptic currents (EPSCs) recorded in type II neurones had 6-cyano-7-nitroquinoxaline-2,3-dione (CNQX)-sensitive fast and D-2-amino-5-phosphonovalerate (APV)-sensitive slow components. The I–V relationship of the fast component showed a strong inward rectification, indicating that inwardly rectifying AMPA receptors are involved in excitatory synaptic transmission.

Among ionotropic receptors of glutamate, a major excitatory neurotransmitter in the central nervous system (CNS), α-amino-3-hydroxy-5-methyl-4-isoxazolepropionic acid (AMPA)-subtype receptor channels mediate fast excitatory synaptic transmission (Nicoll, Malenka & Kauer, 1990; Keller, Konnerth & Yaari, 1991; Ozawa, Iino & Abe, 1991*a*; Seeburg, 1993; Hollmann & Heinemann, 1994). Initially, since the reversal potentials of quisqualate and kainate responses were not affected by raising extracellular Ca^{2+} concentration, the AMPA receptors were considered to be only slightly permeable to Ca^{2+} (MacDermott, Mayer, Westbrook, Smith & Barker, 1986; Mayer & Westbrook, 1987). However, it was later found that AMPA receptors exhibited marked inward rectification and high Ca^{2+} permeability in a population of cultured hippocampal neurones (type II neurones), whereas AMPA receptors exhibited an outwardly rectifying current–voltage (I–V) relationship and little Ca^{2+} permeability in the majority of neurones (type I neurones; Iino, Ozawa & Tsuzuki, 1990; Ozawa, Iino & Tsuzuki, 1991*b*; Ozawa & Iino, 1993). In

* To whom correspondence should be addressed.

addition, a substantial number of neurones exhibited weaker inward rectification than type II neurones. Since the degree of inward rectification in these neurones correlated well with Ca^{2+} permeability, these cells were considered to have a mixed expression of the two types of AMPA receptors with variable ratios (intermediate neurones; Iino, Mochizuki & Ozawa, 1994). A close correlation between the inward rectification and Ca^{2+} permeability of AMPA receptors has also been reported in cultured rat hippocampal neurones by Lerma, Morales, Ibarz & Somohano (1994).

Molecular biological studies have shown that AMPA receptors are composed of subunits taken from a set of four proteins: GluR1 (GluR-A), GluR2 (GluR-B), GluR3 (GluR-C), and GluR4 (GluR-D). They have also shown that the functional properties of AMPA receptors depend on their subunit composition: receptors possessing the GluR2 subunit exhibit either linear or outwardly rectifying I–V relationships and little Ca^{2+} permeability, whereas receptors lacking GluR2 show strong inward rectification and high Ca^{2+} permeability (for reviews, see Seeburg, 1993; Hollmann & Heinemann, 1994). Using a patch-clamp, reverse transcription-polymerase chain reaction (RT-PCR) technique, Bochet *et al.* (1994) have demonstrated that only GluR1 and GluR4 subunits are expressed, and that no GluR2 subunit is detected in type II cultured hippocampal neurones. It is, therefore, likely that CNS neurones regulate Ca^{2+} entry through AMPA receptors by changing their expression of the GluR2 subunit.

To clarify the functional significance of inwardly rectifying and Ca^{2+}-permeable AMPA receptors in the CNS, it is necessary to elucidate their distributions in the CNS and whether they are involved in synaptic transmission. In the hippocampus, AMPA receptors in CA1 and CA3 pyramidal cells (Jonas & Sakmann, 1992) and granule cells (Keller *et al.* 1991) have been shown to display linear or outwardly rectifying I–V relationship (type I response). However, McBain & Dingledine (1993) found a population of interneurones in the stratum radiatum of the CA3 region with inwardly rectifying I–V relationships of kainate-activated current, and suggested that type II neurones are involved in the neural circuit *in situ*. Jonas, Racca, Sakmann, Seeburg & Monyer (1994) have shown that non-pyramidal neurones in the rat visual cortex express Ca^{2+}-permeable AMPA receptors, and that the Ca^{2+} permeability of these AMPA receptors is negatively correlated with the amount of GluR2 expressed in these neurones. Very recently, Koh, Geiger, Jonas & Sakmann (1995) have demonstrated that AMPA receptors expressed in basket cells of rat hippocampal dentate gyrus are highly permeable to Ca^{2+}. In addition, Ca^{2+}-permeable AMPA receptors were found in retinal bipolar cells (Gilbertson, Scobey & Wilson, 1991) and in cerebellar Bergmann glial cells (Burnashev *et al.* 1992; Müller, Möller, Berger, Schnitzer & Kettenmann, 1992). Thus, Ca^{2+}-permeable AMPA receptors appear to be expressed in more various types of cells in the CNS than initially supposed. In the present study, we searched for neurones expressing inwardly rectifying and Ca^{2+}-permeable AMPA receptors in rat hippocampal slices, and examined whether they would be involved in excitatory synaptic transmission.

METHODS

Patch clamp recording in hippocampal slices

Tight-seal patch clamp recording was performed following the method described by Edwards, Konnerth, Sakmann & Takahashi (1989). Briefly, 5- to 13-day-old rats were decapitated, and frontal hippocampal slices 150–220 μm in thickness were prepared with a vibratome (DTK-2000, Dosaka EM, Kyoto, Japan). In the recording chamber, the slices were mounted on the stage of an upright microscope (Axioskop FS, Zeiss, Oberkochen, Germany). Morphologically identified neurones were approached with patch pipettes under visual control, with positive pressure applied to the patch pipette; no cleaning pipette was used. Patch pipettes had a resistance of 3–10 MΩ when filled with internal solution. The series resistance during the recording was typically 8–25 MΩ. An EPC-7 patch clamp amplifier (List, Darmstadt, Germany) was used for voltage-clamp experiments and the pCLAMP system (Axon Instruments) was used for data acquisition and analysis. I–V relationships were obtained by ramping the membrane potential at a rate of 50 mV s^{-1} from −60 to + 60 mV (holding potential −60 mV). Since the liquid-junction potential between the control external solution and the intracellular solution containing CsCl or CsF was estimated as −4 mV, the actual membrane potential was corrected by this value. I–V curves of responses to excitatory amino acids were constructed by subtracting I–V curves obtained in the control solution (the averages of I–V curves obtained before and after application of agonists) from those obtained during application of the agonists. The average of four such trials was routinely presented as an I–V relationship. The membrane input resistance measured from the linear portion of the I–V relationship between −54 and −64 mV in the control solution was 2·2 ± 0·8 GΩ (n = 15, mean ± S.D.) in non-pyramidal neurones. When this value was less than 1·0 GΩ, the neurone was discarded from the experiments.

Conductance–voltage (G-V) plots for responses to kainate and *N*-methyl-D-aspartate (NMDA) were obtained by calculating the conductance values at every 5 mV using the equation:

$$G = I/(V - E_{rev}),$$

where I is the amplitude of the agonist-induced current and E_{rev} is the reversal potential. The plots were normalized with respect to the conductance value at −60 mV (kainate) or +55 mV (NMDA). Data points near the reversal potential were masked.

The agonists were bath-applied. The volume of the bath was 0·5 ml and complete replacement of the external solution was performed by the addition of 2·5 ml of new solution. The flow rate of the bathing solution was 3 ml min^{-1}. Since the volume of the dead space was 0·5 ml, responses to agonists occurred approximately 10 s after switching to the new solution, and reached steady-state responses within another 50 s. In the experiments to estimate Ca^{2+} permeability of the recorded neurones, large nucleated outside-out patches (Sather, Dieudonné,

MacDonald & Ascher, 1992) were obtained by applying slight negative pressure to the patch pipette before pulling away from the somata. *I–V* relationships of the kainate-activated currents were then constructed in Na^+-free, 100 mM Ca^{2+} solution. The large nucleated outside-out patch enabled us to record large current and contributed to enhancement of the signal-to-noise ratio of the recordings. Ca^{2+} permeability was examined in the outside-out rather than whole-cell configuration for the following reasons. Firstly, it was difficult to exclude the possible effect of residual Na^+ in the slices in the case of whole-cell recordings. Secondly, the bath-application of kainate to neurones in the Na^+-free, 100 mM Ca^{2+} solution often caused an increase in the leak conductance of the whole-cell membrane. In the case of outside-out patches, the recording condition was much more stable. We usually changed the slice after the challenge by kainate in this isotonic Ca^{2+} solution.

Excitatory postsynaptic currents (EPSCs) were elicited by applying a voltage pulse of 1–30 V (80–200 μs duration) to a glass pipette containing 2 M NaCl solution (tip diameter was approximately 5 μm; resistance was 1–2 MΩ) placed on the surface of the slice 50–200 μm away from the recorded neurone. In the EPSCs shown, 6–20 records were averaged. Data are expressed as means ± S.D. Statistical evaluation of the results was done with Student's *t* test.

Solutions

The slices were continuously superfused with the control external solution containing (mM): 120 NaCl, 2·5 KCl, 2 $CaCl_2$, 1 $MgCl_2$, 26 $NaHCO_3$, 1·25 NaH_2PO_4, and 25 glucose, bubbled with 95% O_2 and 5% CO_2. Tetrodotoxin (TTX, 500 nM) was added in the experiments with bath application of agonists. In the experiments to measure Ca^{2+} permeability, isotonic Ca^{2+} solution was used containing (mM): 100 $CaCl_2$, 10 glucose, 5 Hepes, and 24 *N*-methylglucamine (pH adjusted to 7·4 with HCl). The internal solution of patch pipettes in most of the experiments contained (mM): 150 CsCl, 5 EGTA, and 10 Hepes (pH adjusted to 7·2 with CsOH). In the experiments to obtain outside-out patches, internal solution containing the following was often used (mM): 130 CsF, 20 CsCl, 5 EGTA, and 10 Hepes (pH adjusted to 7·2 with CsOH). In these internal solutions, using CsOH to adjust pH raised the concentration of Cs^+ by approximately 15 mM. In some experiments, spermine (Sigma) was added to the internal solution. When AMPA was applied as an agonist, 60 μM cyclothiazide (CTZ) (a generous gift from Eli Lilly, Indianapolis, IN, USA) was added to prevent rapid desensitization of AMPA receptors. The simultaneous application of AMPA and CTZ appeared to be toxic to the slices, and we could apply these drugs only once to each preparation. AMPA, kainate, NMDA, 6-cyano-7-nitroquinoxaline-2,3-dione (CNQX), and D-2-amino-5-phosphonovalerate (APV) were purchased from Tocris Cookson (Bristol, UK). Other chemicals were from Sigma.

Intracellular staining

For intracellular staining, whole-cell recording was performed using patch pipettes containing biocytin (Horikawa & Armstrong, 1988). The internal solution contained (mM): 13 biocytin, 120 caesium glucuronate, 20 KCl, 10 EGTA, 2 $MgCl_2$, 2 Na_2ATP, and 10 Hepes (pH adjusted to 7·3 with CsOH). In this case, the liquid-junction potential between the control external solution and the internal solution was −10 mV, and the actual membrane potential was corrected by this value. After patch clamp recording, the patch pipettes were carefully detached from the cell and the slices were fixed overnight in 4% paraformaldehyde solution in 100 mM phosphate-buffered saline (PBS). On the next day, after 2 × 10 min washes in PBS, the slices were incubated in methanol containing 0·6% H_2O_2 for 30 min. After 4 × 5 min washes in PBS, the slices were incubated in avidin–biotin complex solution containing avidin and biotin–horseradish peroxidase solution (Vector Laboratories, Burlingame, CA, USA) and 0·3% Triton X in PBS for 3 h. After 2 × 10 min washes in PBS, the slices were then rinsed with 50 mM Tris-buffered saline (TBS) solution (pH 7·6) for 2 × 10 min, and then incubated in 0·5% $CoCl_2$ solution in TBS for 15 min. After 3 × 5 min washes in TBS, the slices were again rinsed in PBS for 4 × 5 min. The slices were incubated in 0·05% diaminobenzidine (DAB) solution for 30 min and then reacted in the DAB solution containing 0·0025% H_2O_2 for 15 min. After 3 × 5 min washes in PBS solution, the slices were mounted on gelatin-coated slides and air-dried. The slices were counterstained with Nissl stain and coverslipped. Stained cells were traced using a camera lucida at a × 1000 magnification.

RESULTS

Rectification properties of kainate- and AMPA-activated currents

In the uppermost panel of Fig. 1, three different types of *I–V* relationships of responses to kainate, a non-desensitizing agonist for AMPA receptors, in non-pyramidal neurones in the stratum radiatum of the CA1 region of rat hippocampal slices are shown. *I–V* curves were constructed by ramping the membrane potential from −64 to +56 mV during bath application of 200 μM kainate, and the *I–V* relationships of the kainate responses were obtained by subtracting the *I–V* curves in the control solution. The *I–V* relationship in Fig. 1*Aa* exhibited slight outward rectification, whereas that in Fig. 1*Ac* showed marked inward rectification. Although the *I–V* relationship in Fig. 1*Ab* exhibited inward rectification, the degree of rectification was less prominent than that in Fig. 1*Ac*. The reversal potentials were close to 0 mV in these neurones.

To express the degree of inward rectification of current responses of AMPA receptors quantitatively in cultured rat hippocampal neurones, we previously introduced the following value as a rectification index (RI):

$$\mathrm{RI} = [I_{+40} / (40 - E_{\mathrm{rev}})]/[I_{-60} / (-60 - E_{\mathrm{rev}})], \quad (1)$$

where I_{+40} and I_{-60} were the amplitudes of the AMPA- or kainate-induced currents at +40 and −60 mV, respectively, and E_{rev} was the reversal potential (Ozawa *et al.* 1991*b*; Iino *et al.* 1994). When these values were $>1{\cdot}0$ and $<0{\cdot}25$ in the control solution, we assigned the responses to the type I and type II categories, respectively. In the case of $0{\cdot}25 \leqslant \mathrm{RI} \leqslant 1{\cdot}0$, the response was classified as an intermediate type (Iino *et al.* 1994). Accordingly, neurones with $\mathrm{RI} > 1{\cdot}0$, $\mathrm{RI} < 0{\cdot}25$, and $0{\cdot}25 \leqslant \mathrm{RI} \leqslant 1{\cdot}0$ were referred to as type I, type II and intermediate neurones, respectively. We used the same designation for neurones in hippocampal slices in this paper. The RI values in Fig. 1*Aa*, *Ba* and *Ca* were 1·16, 0·79 and 0·24, and the neurones

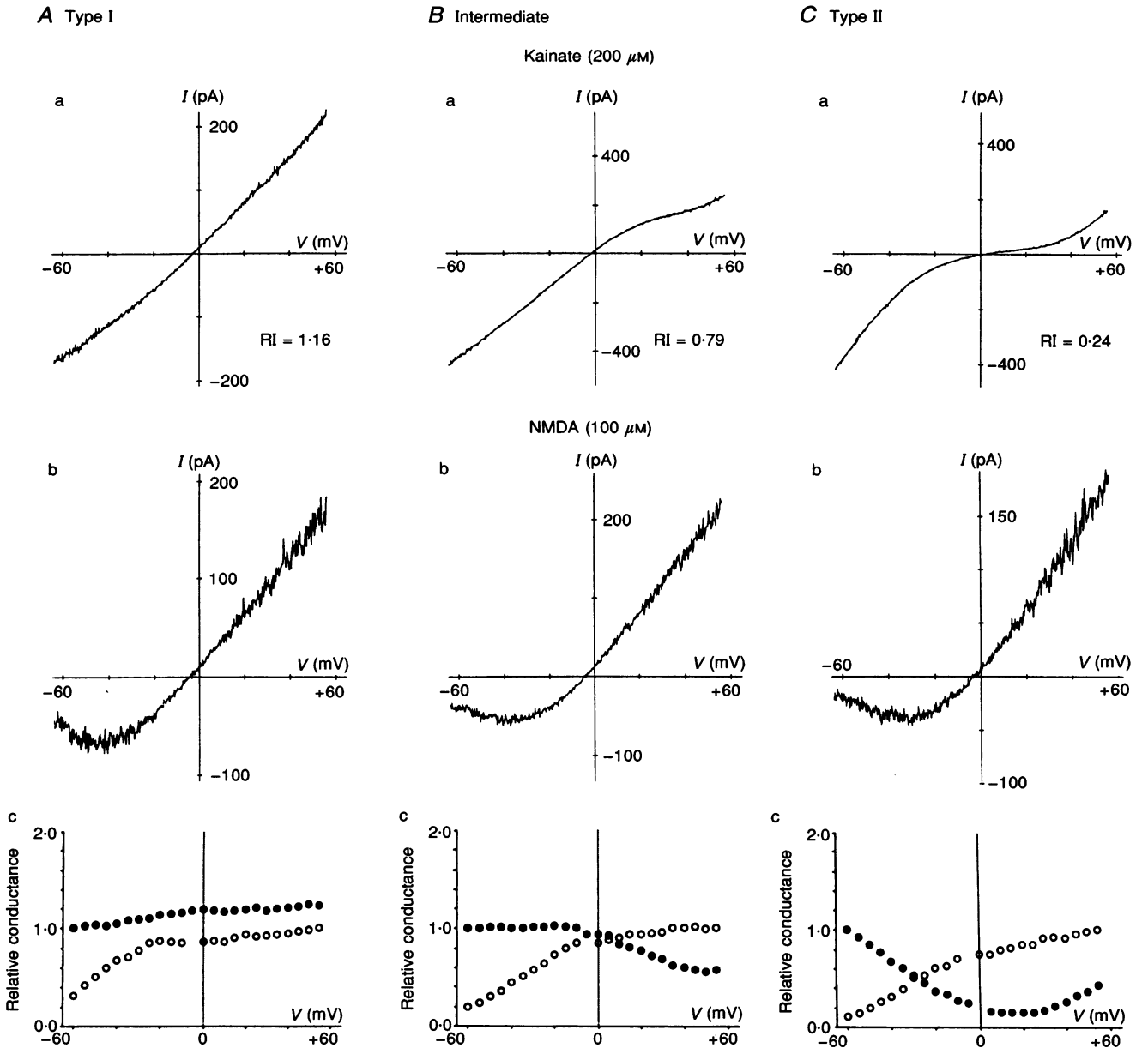

Figure 1. Three types of whole-cell *I–V* relationships of kainate responses obtained in non-pyramidal neurones

In *A–C*, the uppermost panel (*a*) shows the whole-cell *I–V* relationships of kainate (200 μM) responses in three types of non-pyramidal neurones in the stratum radiatum of the CA1 region of the hippocampus. *A*, a type I neurone with outwardly rectifying *I–V* relationship (RI = 1·16). *B*, an intermediate neurone with weak inward rectification (RI = 0·79). *C*, a type II neurone with strong inward rectification (RI = 0·24). These *I–V* relationships were constructed by subtracting *I–V* curves obtained in the control solution from those obtained during application of the agonist. The membrane potential was ramped from −64 to +56 mV. The middle panel (*b*) in *A–C* shows the whole-cell *I–V* relationships of NMDA (100 μM) responses in these three types of neurones. The lowermost panel (*c*) indicates conductance–voltage plots for both kainate- (●) and NMDA-activated conductances (○), obtained from the *I–V* relationships shown in the uppermost and middle panels, respectively. Normalized values with respect to the conductance value at −60 mV (kainate) or +55 mV (NMDA) are plotted at every 5 mV between −60 and +55 mV. The conductance–voltage plots for kainate-activated conductance illustrate marked differences in the rectification properties of kainate responses in the three types of neurones, whereas those of NMDA responses are similar.

showing these I–V relationships of kainate responses were designated as type I, intermediate and type II neurones, respectively. The reversal potentials of type I, type II and intermediate neurones were $-3{\cdot}6 \pm 3{\cdot}7$ mV (mean ± S.D., $n = 217$), $-3{\cdot}0 \pm 4{\cdot}2$ mV ($n = 66$), and $-3{\cdot}5 \pm 4{\cdot}8$ mV ($n = 247$), respectively.

The type I, type II and intermediate neurones were almost equally sensitive to NMDA. The middle panel of Fig. 1 shows the I–V relationships of responses to 100 μM NMDA applied to the same neurones giving the three distinct types of I–V relationships of kainate responses. The shapes of I–V relationships of NMDA responses showed similar outward rectification at potentials more positive than −24 mV both in the type II and intermediate neurones as seen in the type I neurones. This indicates that the inward rectification of kainate responses detected in the type II and intermediate neurones was not an artifact due to poor control of the membrane potential. Conductance–voltage plots for both kainate and NMDA-activated conductances in the three types of neurones are shown in the lowermost panel of Fig. 1. These plots clearly reveal marked differences in the voltage dependence of kainate-activated conductances in the three types of neurones. In contrast, the voltage dependence of NMDA-activated conductances was similar among these neurones.

Kainate is an agonist not only of AMPA receptors, but also of high-affinity kainate receptors composed of GluR5, GluR6, GluR7, KA-1 and/or KA-2 subunits (Seeburg, 1993; Hollmann & Heinemann, 1994). It has been demonstrated that both cloned and native high-affinity kainate receptors show pronounced desensitization with fast onset and slow recovery, and produce very little steady-state response to prolonged application of kainate in the absence of concanavalin A (Egebjerg, Bettler, Hermans-Borgmeyer & Heinemann, 1991; Lerma, Paternain, Naranjo & Mellström, 1993; Partin, Patneau, Winters, Mayer & Buonanno, 1993). Since the I–V relationships of kainate responses shown in Fig. 1 were obtained in the steady state during bath application of kainate, it is likely that these were predominantly due to the activation of AMPA receptors. To confirm this, we occasionally used 100 μM AMPA together with 60 μM cyclothiazide (CTZ), which prevents fast desensitization of AMPA receptors (Partin *et al.* 1993), instead of kainate to activate AMPA receptors. All neurones tested (5 type I, 17 intermediate and 5 type II neurones) showed the same types of I–V relationships of responses to both AMPA (plus CTZ) and kainate (data not shown). However, the simultaneous application of AMPA and CTZ appeared to be toxic to hippocampal slices, and we failed to obtain reasonable patch clamp recordings after slices had been challenged once by these drugs. Therefore, we used kainate to activate AMPA receptors in the present experiments.

Rectification and Ca^{2+} permeability of AMPA receptors

To estimate the Ca^{2+} permeability of the recorded neurones, a large nucleated outside-out patch (Sather *et al.* 1992) was made and the I–V relationship of the kainate-activated current was obtained in the Na^+-free extracellular solution containing 100 mM Ca^{2+} after the whole-cell I–V relationship of AMPA receptors had been determined in the control solution. Figure 2 shows the I–V relationships of the kainate-activated currents in Na^+-free, 100 mM Ca^{2+} solution in the three types of neurones. The reversal potential of type I neurones ranged between −20 and −61 mV ($n = 7$, mean ± S.D. $= -44{\cdot}4 \pm 14{\cdot}0$ mV; Fig. 2*A*). The value of P_{Ca}/P_{Cs}, the ratio of the permeability coefficient of Ca^{2+} and Cs^+ and estimated according to the constant-field equation (see Iino *et al.* 1990), was 0·08. On the other hand, the reversal potential of type II neurones ranged from +8 to +17 mV ($n = 5$, mean ± S.D. $= +11{\cdot}8 \pm 3{\cdot}6$ mV; Fig. 3*C*), indicating that the value of P_{Ca}/P_{Cs} was 1·71. In addition, the reversal potential of intermediate neurones ranged from +2 to −18 mV ($n = 7$, mean ± S.D. $= -8{\cdot}7 \pm 7{\cdot}4$ mV) and was between those of the type I and type II neurones as shown in Fig. 2*B*. The mean value of P_{Ca}/P_{Cs} in the intermediate neurones was 0·50.

During the course of these experiments, we noticed that the inward rectification of the AMPA receptor in type II neurones was lost gradually in the outside-out patch configuration and the I–V relationship of the kainate response became almost linear or even outwardly rectifying by the time the Ca^{2+} permeability was measured (Fig. 2*C b*). It has been shown that the inward rectification of the Ca^{2+}-permeable AMPA receptor is lost gradually in outside-out patches obtained from type II hippocampal neurones in culture, and that this loss of the inward rectification is not accompanied by a change in the Ca^{2+} permeability (Isa, Iino, Itazawa & Ozawa, 1995). The inward rectification in the outside-out patch is maintained stably by applying spermine to the cytoplasmic side of the patch membrane. Furthermore, this effect of spermine is specific for the AMPA receptor in type II neurones in culture, and spermine exerts no influence on the rectification properties of the AMPA receptor in type I hippocampal neurones. This was also the case for the AMPA receptor in type II neurones in hippocampal slices. When 300 μM spermine was added to the internal solution filling the patch pipette, the inward rectification of the AMPA receptor in the cell-free patch was maintained with no change in the reversal potential (Fig. 2*D*). Very recently, several reports have appeared showing that the inward rectification of Ca^{2+}-permeable non-NMDA glutamate receptors is lost in outside-out patches and the inclusion of spermine in the internal solution prevents the loss of the rectification both in native and recombinant receptors

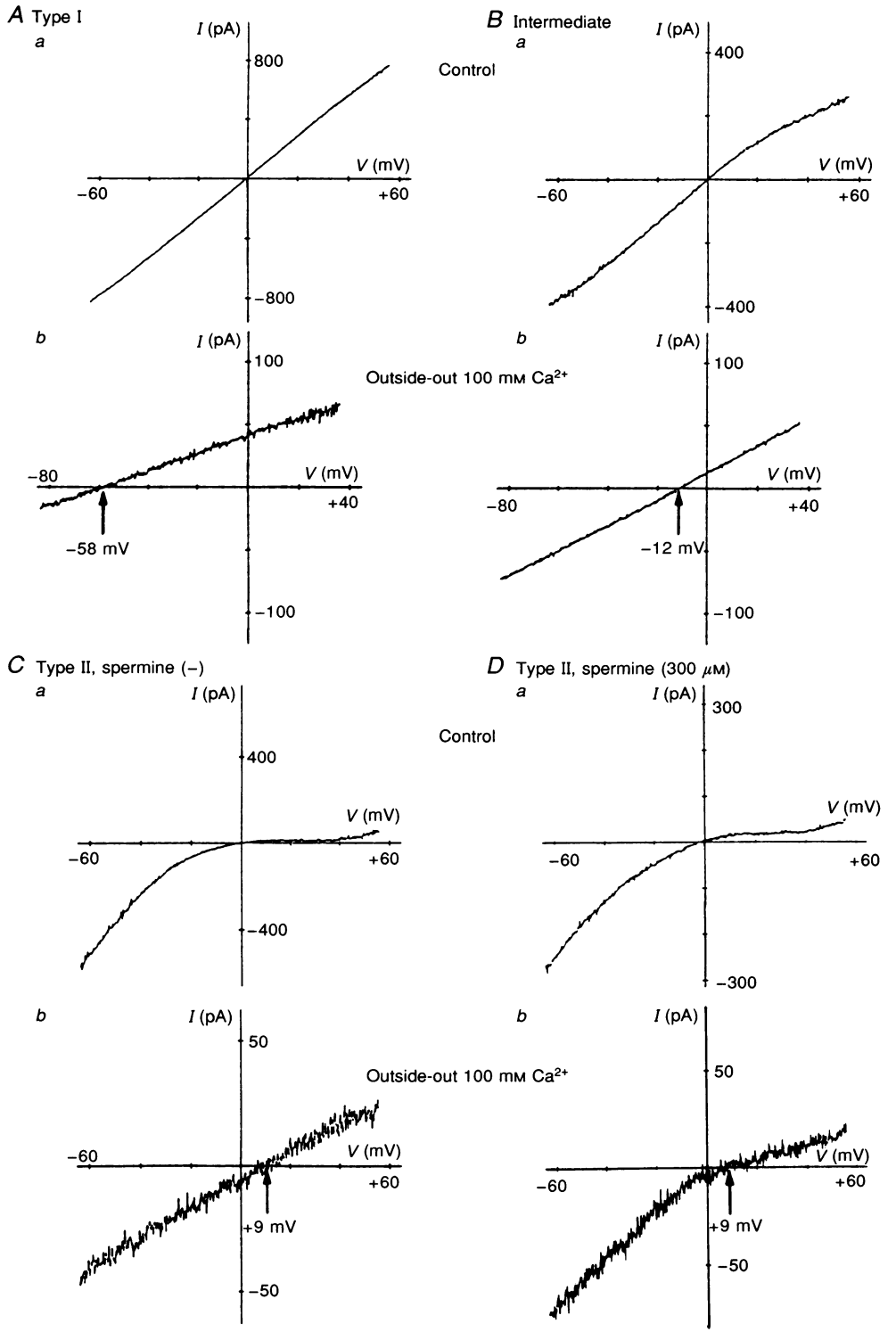

Figure 2. Ca^{2+} permeability of AMPA receptors in the three types of hippocampal neurones

A–C, upper panel, *I–V* relationships of the whole-cell kainate (200 μM) responses between −64 and +56 mV obtained in control solution. Lower panel, *I–V* relationships of kainate responses in large nucleated outside-out patches (bathed in isotonic Ca^{2+} solution containing 100 mM Ca^{2+}) excised from the somatic regions of the neurones of which *I–V* relationships of the whole-cell kainate responses are shown in the upper panel. *A–C*, *I–V* relationships from type I, intermediate and type II neurones, respectively. *D*, *I–V* relationships from a type II neurone examined with the use of a patch pipette filled with the internal solution containing 300 μM spermine. Upper panel, *I–V* relationship of kainate responses in the whole-cell configuration; lower panel, in the outside-out patch in the isotonic Ca^{2+} solution. Note that inward rectification is maintained in the outside-out patch in this case.

(Kamboj, Swanson & Cull-Candy, 1995; Koh, Burnashev & Jonas, 1995; Bowie & Mayer, 1995; Donevan & Rogawski, 1995).

Figure 3 shows scatter plots between the RI obtained in the whole-cell recording and the reversal potential value of kainate response in the outside-out patch in the Na^+-free, 100 mM Ca^{2+} solution. The data obtained without spermine in the patch-pipette and those with 300 μM spermine are plotted with filled and open circles, respectively. These plots indicate a close correlation between the degree of inward rectification of the whole-cell kainate response and the Ca^{2+} permeability of AMPA receptors in hippocampal neurones in slices, as shown previously in cultured hippocampal neurones (Iino *et al.* 1994). The Ca^{2+} permeability of AMPA receptors was unaffected by internal spermine also in hippocampal neurones in slices. When the internal solution contained 300 μM spermine, the reversal potentials of kainate responses in the outside-out patch in the Na^+-free, 100 mM Ca^{2+} solution were $-46{\cdot}3 \pm 11{\cdot}9$ mV ($n = 3$) and $+10{\cdot}8 \pm 1{\cdot}6$ mV ($n = 5$) in type I and type II neurones, respectively. This indicates that the mean values of P_{Ca}/P_{Cs} are 0·08 and 1·60 in type I and type II neurones, respectively, being similar to the corresponding values estimated by using patch pipettes containing no spermine in both types of neurones.

Distribution of type I, type II and intermediate neurones in the hippocampus

The *I–V* relationships of the whole-cell kainate responses were obtained in a total of 665 neurones located in various parts of the hippocampus. Figure 4 shows the distribution of RI of the cells recorded in the respective regions. As shown in Fig. 4*A*, the majority of pyramidal cells in the CA1 region showed type I responses (42/49, 86%). Some neurones (7/49, 14%) belonged to the intermediate type, but their RI values were relatively close to 1·0 (0·77–0·98). In contrast, a considerable number of non-pyramidal neurones in the stratum pyramidale (SP) of the CA1 region belonged to the intermediate type (11/36, 31%). RI of the intermediate type ranged from 0·31–0·94 in this class of neurones. On the other hand, type I, type II, and intermediate neurones comprised 28% (44/156), 25% (39/156) and 47% (73/156), respectively, of the neurones in the stratum radiatum (SR) and stratum lacunosum-moleculare (SLM). In the CA3 region, 61% (11/18) and 39% (7/18) of the pyramidal cells in the CA3 region were type I and intermediate (Fig. 3*D*), respectively. The proportion of intermediate type cells was slightly higher in the CA3 than in the CA1 pyramidal neurones. On the other hand, 40% (15/38), 13% (5/38), and 47% (18/38) of non-pyramidal neurones in the SP and the stratum lucidum of the CA3 region were type I, type II and intermediate type, respectively. Among the non-pyramidal neurones in SR and SLM of the CA3 regions, 40% (118/294), 12% (34/294), and 48% (142/294) were type I, type II and intermediate type, respectively. In summary, the proportion of neurones expressing inwardly rectifying AMPA receptors (type II and the intermediate) was relatively high in the SR and SLM in both CA1 and CA3 regions. They were also distributed in a substantial population of neurones in the SP. In the dentate gyrus, type I, type II, and intermediate neurones comprised 76% (25/33), 3% (1/33), and 21% (7/33), respectively, in the stratum granulosum (SG) (granule cells and other interneurones were counted together, because it was impossible to differentiate between them on the basis of their appearance only). In the hilus (HL), type I, type II, and intermediate neurones comprised 82% (14/17), 12% (2/17) and 6% (1/17), respectively. In the stratum moleculare (SM), these types of neurones comprised 42% (10/24), 20% (5/24), and 38% (9/24), respectively. Thus, the proportion of neurones expressing inwardly rectifying AMPA receptors (type II and intermediate) in the dentate gyrus was higher in the SM than in the SG and hilus.

Morphological properties of neurones expressing inwardly rectifying AMPA receptors

A total of sixty-nine non-pyramidal neurones were stained with biocytin. Among them, twenty-eight, seventeen and twenty-four were type I, type II and intermediate neurones, respectively. Figure 5 illustrates the morphology of type II neurones. Figure 5*A* and *C* show a photomicrograph and a camera lucida drawing, respectively, of a biocytin-stained type II neurone in the SR of the CA1 region. The *I–V* relationship of the whole-cell kainate

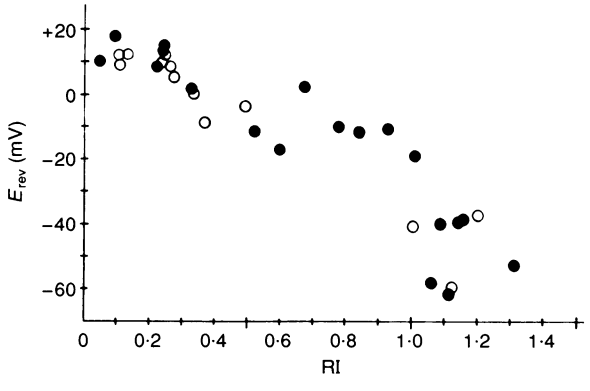

Figure 3. Scatter plots of reversal potentials of kainate responses in outside-out patches bathed in isotonic Ca^{2+} solution against RI values obtained in the whole-cell configuration

Plots obtained with the use of patch pipettes containing no spermine are indicated by ● ($n = 19$), and those with patch pipettes containing 300 μM spermine are indicated by ○ ($n = 13$). Note that the degree of inward rectification of the whole-cell kainate responses correlates closely with the Ca^{2+} permeability in the outside-out patch excised from the same cell both in the absence and presence of spermine in the patch pipette.

response in this neurone is shown in Fig. 5*B* (RI = 0·23). The soma of this neurone was ellipsoidal and projected a few dendrites. An axon (arrow) projected towards the SP, and then turned back to the SR. Figure 5*D–G* show camera lucida drawings of four other type II neurones located in various parts of the hippocampus. The neurone in Fig. 5*D* projected an axon towards the SR, which showed divergent branching in this area. The neurone in Fig. 5*E* was located at the edge of the SP of the CA3 region and issued axonal projections and terminated in the SR. The neurone in

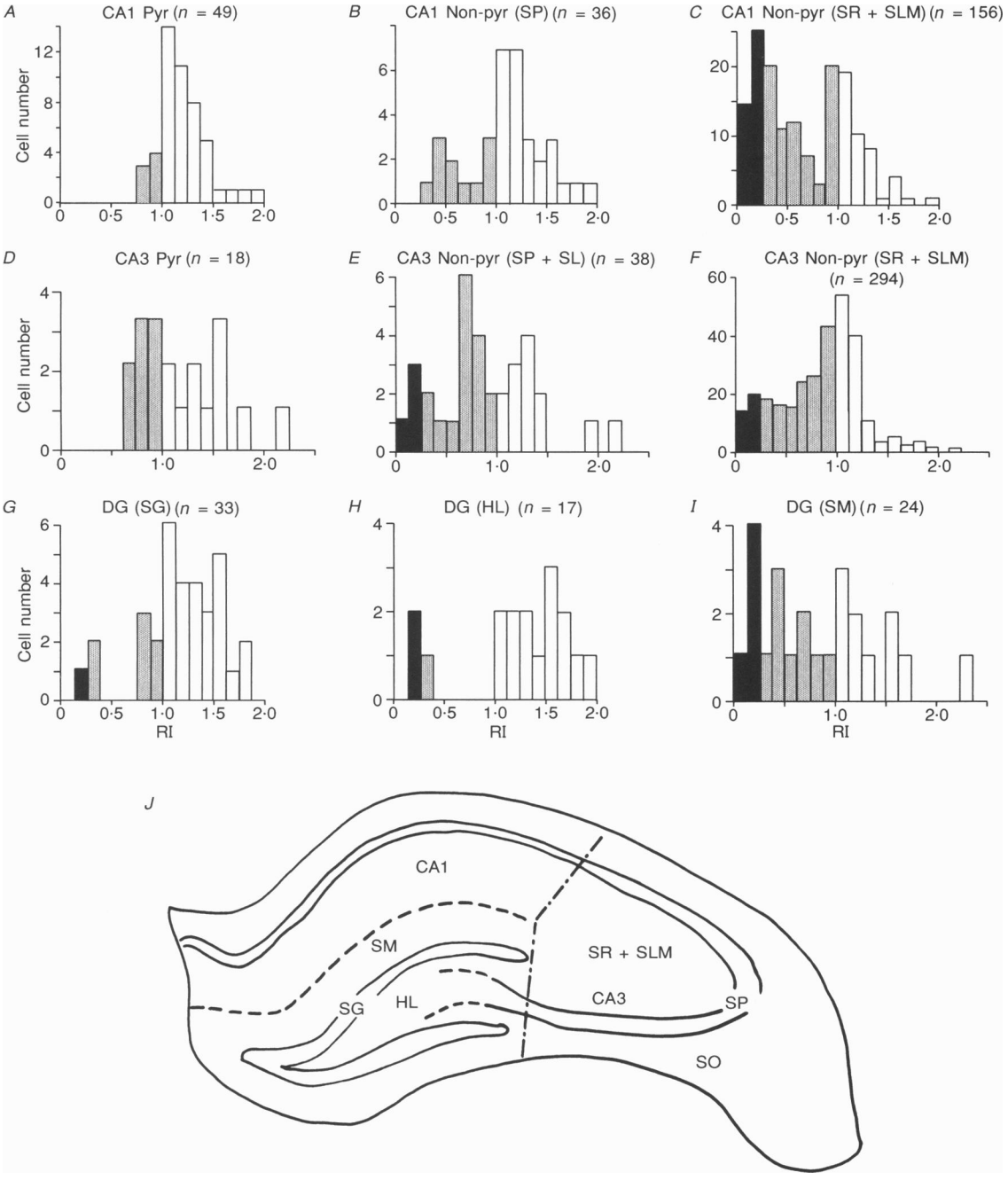

Figure 4. Distribution of inwardly rectifying AMPA receptors in various regions of the hippocampus

A–I, frequency histograms of RI values of neurones recorded in each region of the hippocampus. □, ▨ and ■, type I, intermediate and type II neurones, respectively. *J*, schematic drawing of the hippocampus, indicating the anatomical location of each region. Pyr, pyramidal cells; Non-pyr, non-pyramidal cells; SP, stratum pyramidale; SR, stratum radiatum; SLM, stratum lacunosum-moleculare; SL, stratum lucidum; DG, dentate gyrus; SG, stratum granulosum; HL, hilus; SM, stratum moleculare; SO, stratum oriens. In the CA3 region, the SL was included in the SP.

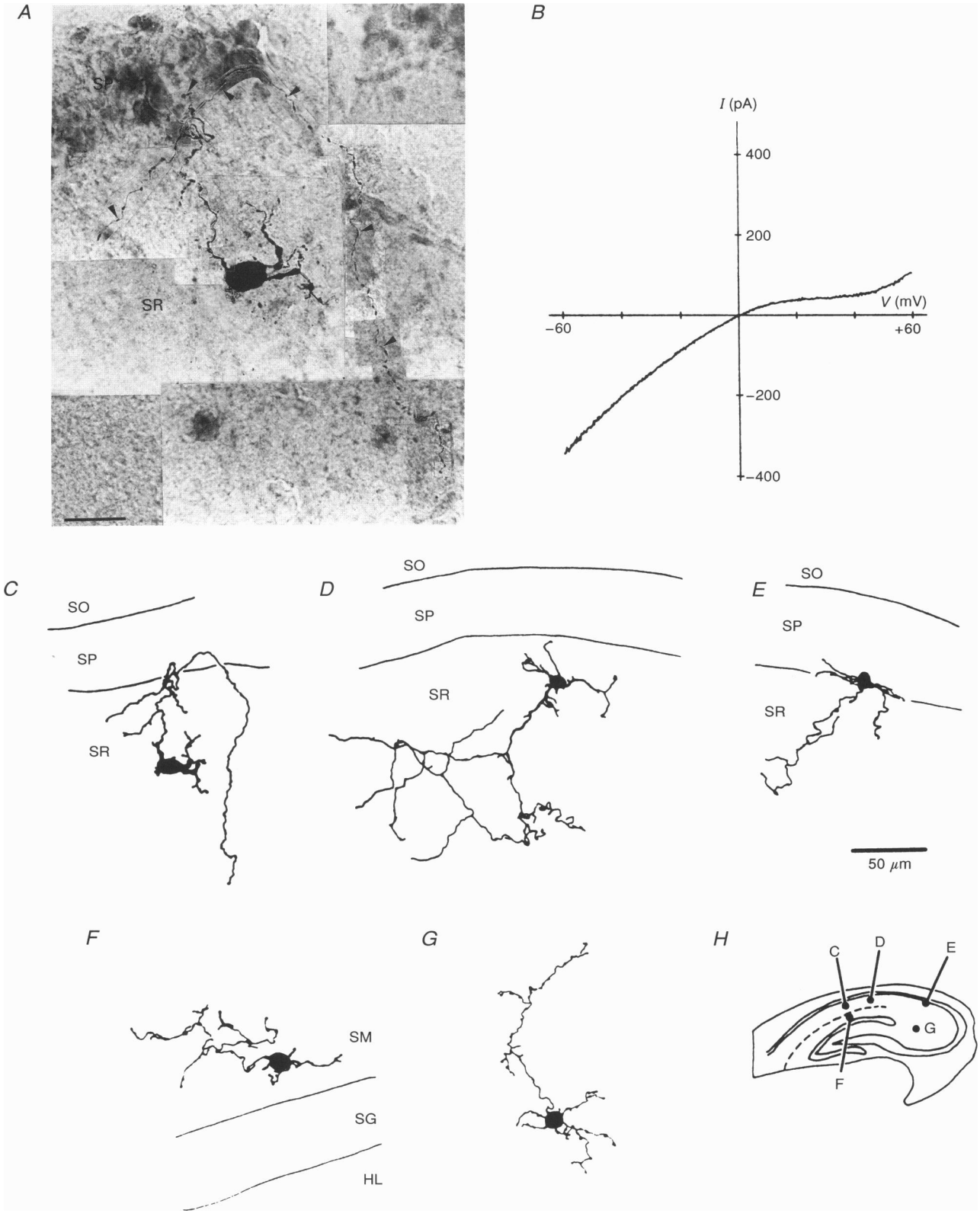

Figure 5. Morphology of type II neurones

A, photomicrograph of a biocytin-stained type II neurone in the SR of the CA1 region and its neurite projections. Arrows indicate the axon. Scale bar: 20 μm. *B*, *I–V* relationship of the whole-cell kainate response of the neurone shown in *A*. *C–G*, camera lucida drawings of 5 type II neurones. Thickness of the slices is 180 μm. The neurone in *C* is the same as that in *A*. *H*, locations of the neurones in *C–G* are plotted on a frontal plane of the hippocampus.

Fig. 5*F* was located in the SM of the dentate gyrus, issued axonal projections and apparently terminated in the dendritic layers of the granule cells. The neurone in Fig. 5*G* issued axonal projections and terminated in the SR of the CA3 region. Thus, the type II neurones appeared to exert synaptic effects on neurones in the surrounding regions. The locations of the five type II neurones are indicated in Fig. 5*H*. The somata of the type II neurones were round or ellipsoidal in shape. However, no clear difference in the shapes of the somata was found among type I, type II and intermediate non-pyramidal neurones. Somatic diameters of stained type I, type II and the intermediate non-pyramidal neurones were (11·3 ± 2·1 μm) × (8·8 ± 1·8 μm) ($n = 28$), (10·8 ± 1·7 μm) × (8·5 ± 1·3 μm) ($n = 17$), and (11·2 ± 1·3 μm) × (9·2 ± 1·5 μm) ($n = 24$) (mean ± S.D.), respectively. There were no significant differences ($P > 0·05$) among their somatic diameters.

Figure 6 shows camera lucida drawings of two examples of intermediate neurones. Figure 6*A* shows an intermediate neurone (RI = 0·76; Fig. 6*A c*) located in the SP of the CA3 region. The location is shown in Fig. 6*A b*. This neurone showed extensive axonal projection chiefly inside the SP, and its axons could be traced for more than 250 μm within the single 180 μm-thick slice. Figure 6*B* shows another intermediate neurone (RI = 0·51; Fig. 6*B c*). The location is shown in Fig. 6*B b*. As shown in Fig. 6*B a*, this neurone projected its axons towards the SP and into the SR with a large number of branchings.

Involvement of inwardly rectifying AMPA receptors in excitatory synaptic transmission

To clarify whether the inwardly rectifying AMPA receptors are involved in excitatory synaptic transmission, *I–V* relationships of the EPSCs were investigated in type II neurones after identification of the neurone type by constructing the *I–V* relationship of the kainate-activated whole-cell current (Fig. 7*D*). Figure 7*A* shows the EPSCs recorded at various membrane potentials in a type II neurone located in the SR of the CA1 region. The EPSCs were evoked by stimulation of a point in the SR approximately 80 μm distant from the soma in the control solution containing 10 μM bicuculline methobromide (Bic), and consisted of two distinct components. The slow

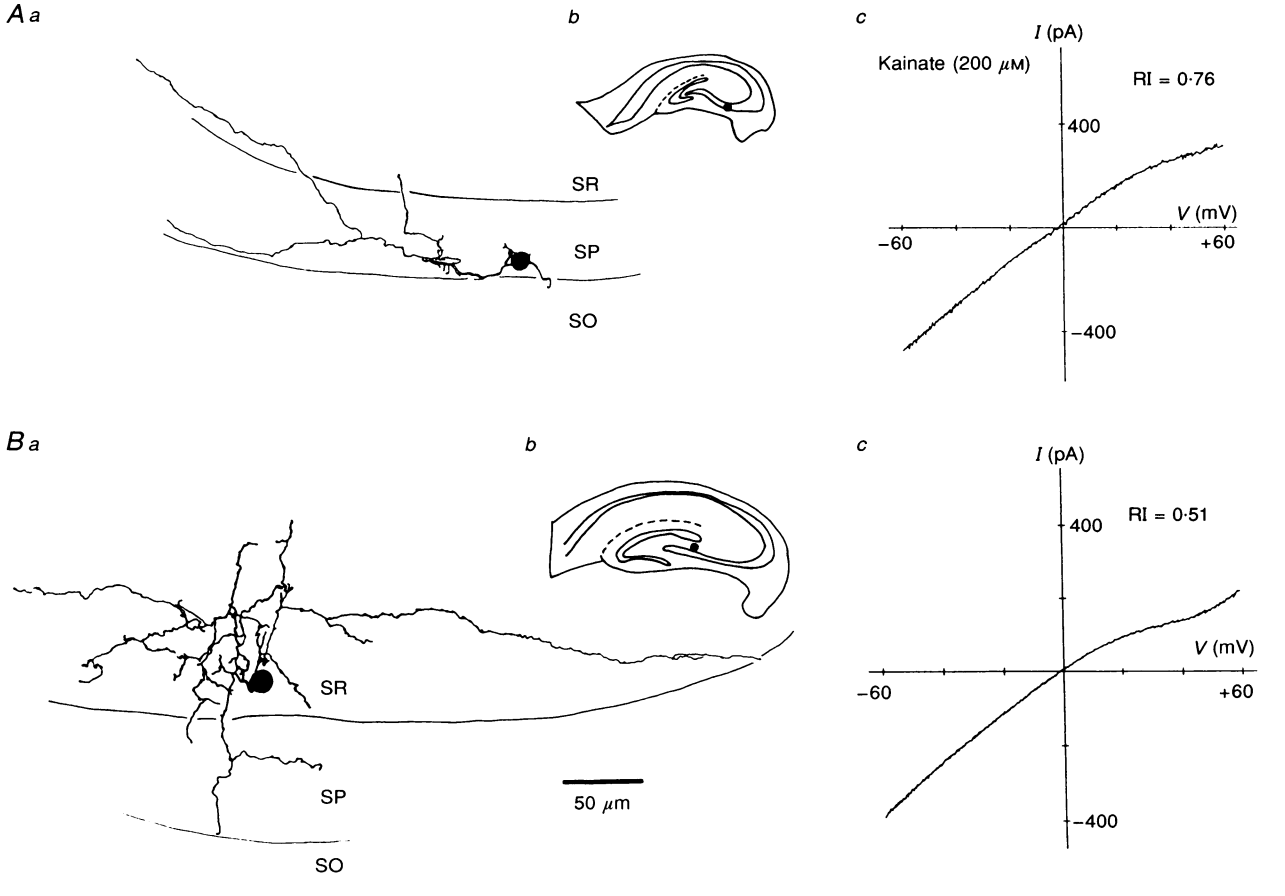

Figure 6. Morphology of intermediate neurones

A a, camera lucida drawing of an intermediate neurone in the SP of the CA3 region. The location of the soma is shown in *A b* and the *I–V* relationship of the whole-cell kainate response is shown in *A c*. *B*, another intermediate neurone in the SR of the CA3 region.

component was abolished by application of 50 μM APV (Fig. 7*A* and *B*). It was more prominent at more positive potentials, and the *I–V* relationship measured 14·7 ms after the stimulus showed a J-shape with a negative slope conductance at potentials more negative than −24 mV (triangles in Fig. 7*A* and *C*). The fast component was unaffected by 50 μM APV (Fig. 7*B*), but was abolished completely by 5 μM CNQX (data not shown). Thus, the EPSCs were generated by activation of both AMPA and NMDA receptors in type II neurones.

Figure 7*C* shows plots of the amplitudes of the fast components of EPSCs, the amplitude measured at 2·9 ms after the stimulus in the control solution (■) and the peak amplitude in the presence of 50 μM APV (●), against the membrane potential. The two *I–V* relationships were similar, and showed strong inward rectification (RI = 0·16, in the presence of APV). Similar results were obtained in the EPSCs evoked in five other type II neurones. These results indicate that the inwardly rectifying AMPA receptors are involved in excitatory synaptic transmission.

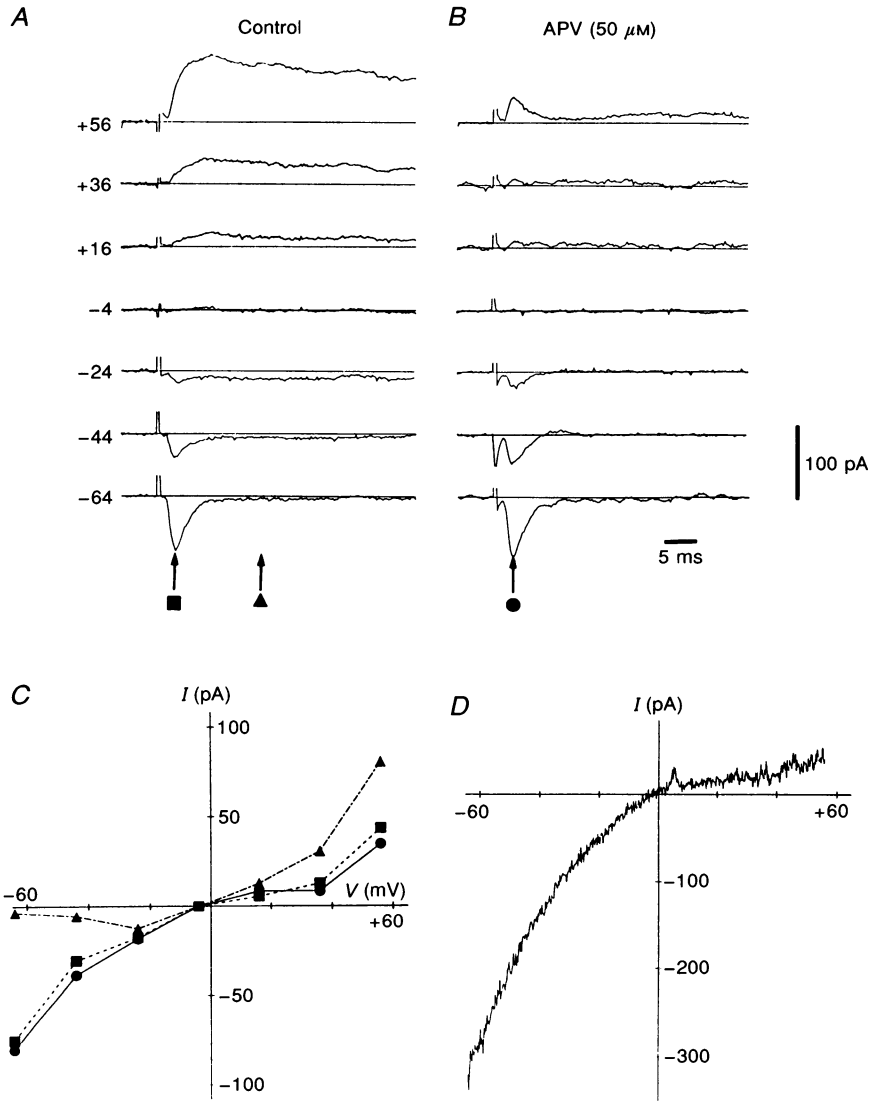

Figure 7. EPSCs recorded in a type II neurone in the stratum radiatum of the CA1 region

A, EPSCs recorded at various membrane potentials between −64 and +56 mV in 20 mV steps in control solution containing 10 μM bicuculline methobromide (Bic). Bic was added in order to block synaptic activities mediated by GABA. Stimulation of the presynaptic fibres was applied at a point 80 μm distant from the soma. *B*, EPSCs recorded during addition of 50 μM APV. *C*, *I–V* relationships of EPSCs. ■ and ▲, amplitudes of EPSCs at 2·9 and 14·7 ms following the stimuli, respectively, in *A*. ▲, mainly EPSCs generated by activation of NMDA receptors. ●, amplitude of EPSCs at 2·9 ms in *B*, which represents the EPSCs generated by activation of AMPA receptors. *D*, *I–V* relationship of the whole-cell response to kainate (200 μM) obtained in the same neurone before recording EPSCs.

DISCUSSION

Inward rectification and Ca^{2+} permeability of AMPA receptors

It has been demonstrated that a population of hippocampal neurones in culture (type II neurones) expresses AMPA receptors with a strong inward rectification and a high Ca^{2+} permeability (Iino *et al.* 1990; Ozawa *et al.* 1991*b*). These cultured type II neurones have been shown to lack the GluR2 subunit (Bochet *et al.* 1994). In the present study, we found that a substantial number of non-pyramidal neurones in rat hippocampal slices had AMPA receptors with strong inward rectification. Since the degree of the inward rectification correlated closely with the Ca^{2+} permeability, the AMPA receptors with strong inward rectification were considered to be highly permeable to Ca^{2+}. McBain & Dingledine (1993) classified interneurones in the SR of the CA3 region of the rat hippocampus into two types, type I and type II interneurones, on the basis of the *I–V* relationship of the whole-cell kainate response and the kinetic properties of spontaneous mEPSCs. They suggested that the type II interneurones express inwardly rectifying and Ca^{2+}-permeable AMPA receptors that lack the GluR2 subunit. In general, the present study corroborated their conclusion, the only difference being that a clear outward current was detected here at potentials more positive than +40 mV in the type II neurones, as was seen previously in type II hippocampal neurones in culture (Ozawa *et al.* 1991*b*). On the other hand, no outward current was detected up to +60 mV in type II interneurones by the previous authors (McBain & Dingledine, 1993). The reason for this discrepancy is presently unknown.

Loss of the inward rectification of Ca^{2+}-permeable AMPA receptors in the outside-out patch

It has been shown that the Ca^{2+} permeability of AMPA receptors is markedly higher in non-pyramidal neurones than pyramidal cells in the rat visual cortex when examined in the outside-out patch configuration, and that the level of GluR2 subunit expression is significantly lower in non-pyramidal neurones (Jonas *et al.* 1994). Apparently, the functional properties of Ca^{2+}-permeable AMPA receptors in the outside-out patch derived from non-pyramidal neurones of the neocortex are different from those of recombinant AMPA receptors lacking the GluR2 subunit in that the *I–V* relationship of AMPA receptors from the neocortical non-pyramidal neurones is only weakly rectifying (Jonas *et al.* 1994). In the present experiments, the *I–V* relationship of Ca^{2+}-permeable AMPA receptors displayed no prominent inward rectification in the outside-out patch in type II hippocampal neurones in slices, whereas the rectification was remarkable when examined in the whole-cell configuration. This uncoupling of the inward rectification from Ca^{2+} permeability in the outside-out patch could be accounted for by the dissipation of intracellular factors conferring the rectification on Ca^{2+}-permeable AMPA receptors. Very recently, it has been shown that the inward rectification is lost in the outside-out patch and the loss of the rectification is prevented by including spermine in the patch-pipette in Ca^{2+}-permeable non-NMDA receptors (Kamboj *et al.* 1995; Koh *et al.* 1995; Bowie & Mayer, 1995; Donevan & Rogawski, 1995; Isa *et al.* 1995). Several pieces of evidence suggest that spermine is a strong candidate for the intracellular factor mediating the inward rectification (Kamboj *et al.* 1995; Bowie & Mayer, 1995). In the present experiments, the inward rectification of kainate responses in outside-out membrane patches derived from type II neurones in hippocampal slices was also rescued by internal spermine (Fig. 2*C* and *D*). This result strongly suggests that intracellular spermine regulates the rectification properties of Ca^{2+}-permeable AMPA receptors in type II neurones in slices.

We often encountered type II neurones in which the degree of the inward rectification of AMPA receptors was attenuated during long-lasting whole-cell recording. This is probably due to slow dissipation of the intracellular rectification factor. However, this attenuation of the inward rectification occurred in a much slower time course in the whole-cell configuration as compared with that in the cell-free patch. To calculate the RI value, we always obtained the *I–V* relationship of kainate response immediately after the patch membrane was disrupted, and usually the RI value was stable for at least 5 min in the whole-cell configuration. Therefore, we believe that the estimation of the RI value in the present experiments is not seriously influenced by the dialysis of each neurone in the whole-cell recording conditions. This notion is supported by the fact that the RI value estimated in the whole-cell configuration in type II neurones in slices was not reduced significantly by adding 300 μM spermine to the internal solution (see Fig. 3).

Subunit composition and location of inwardly rectifying and Ca^{2+}-permeable AMPA receptors

Using a single-cell RT-PCR technique, Bochet *et al.* (1994) have revealed that only GluR1 and GluR4 are expressed and no GluR2 is detected in type II hippocampal neurones in culture. They have also shown that the flop splicing variant is overwhelmingly dominant for both the GluR1 and GluR4 subunits in these cells. An obvious question is whether the inwardly rectifying and Ca^{2+}-permeable AMPA receptors in type II neurones in hippocampal slices have the same subunit composition as those in cultured type II neurones. The regional distribution of each AMPA receptor subunit in the brain has been studied extensively by *in situ* hybridization (Keinänen *et al.* 1990; Sommer *et al.* 1990; Monyer, Seeburg & Wisden, 1991). However, these studies do not provide useful clues to answer this question, since the type II neurones are distributed sparsely throughout the hippocampus and intermingled with other

types of neurones, and the *in situ* hybridization studies do not allow one to determine the subunit composition of receptors at the single cell level. Using a single-cell RT-PCR technique, Geiger *et al.* (1995) have recently determined relative abundance of AMPA receptor subunit mRNA in nine different cell types of rat brain slices. Their results suggest that differential expression of GluR2 and GluR4 accounts for the differences in Ca^{2+} permeability and gating properties of AMPA receptors in those cells. With regard to hippocampal neurones, they have conducted the analyses for CA3 pyramidal cells, hilar mossy cells, hilar interneurones and dentate granule and basket cells. Similar analyses for type II neurones described in the present study remain to be conducted.

It has been shown that desensitization of responses to glutamate is strongly attenuated by CTZ for recombinant AMPA receptors formed from the flip splice variants, whereas it remained pronounced but with slower time course for those from the flop variants (Partin, Patneau & Mayer, 1994). This observation has led to a suggestion that CTZ can be used as a pharmacological tool to distinguish between native AMPA receptors containing flip *versus* flop subunits. In the present study, we failed to observe pronounced desensitization of responses to co-applications of AMPA and CTZ in type II neurones in slices. However, this does not necessarily mean that AMPA receptors in these neurones are formed from the flip variants, since the drugs were bath-applied with a slow perfusion rate that might not allow detection of the desensitization. It would provide useful information about the subunit composition (flip *versus* flop) of AMPA receptors in type II neurones in slices to examine the effects of CTZ on the desensitization of AMPA responses using a rapid drug application method.

Very recently, it has been shown that no major differences are found in the functional properties of both AMPA and NMDA receptors between somatic and dendritic patches derived from CA1 and CA3 pyramidal neurones of the hippocampus (Spruston, Jonas & Sakmann, 1995). This result has led to a suggestion that synaptic and extrasynaptic AMPA or NMDA receptor channels have similar properties, since at least some of the channels on the dendrites seem to be from subsynaptic membrane. This is consistent with the observation in this study that the inwardly rectifying AMPA receptors are presumably present on both the subsynaptic membrane of the dendrites and the extrasynaptic membrane of the soma.

Functional significance of inwardly rectifying and Ca^{2+}-permeable AMPA receptors

The present study has shown that type II and intermediate neurones carrying inwardly rectifying and Ca^{2+}-permeable AMPA receptors (type II AMPA receptors) are abundantly distributed in various areas of the hippocampus. Morphological analysis suggested that most of type II and intermediate neurones are interneurones. Cultured type II hippocampal neurones have been demonstrated to express mRNA for glutamic acid decarboxylase (GAD), and thus to be GABAergic interneurones (Bochet *et al.* 1994). It has also been shown that non-pyramidal neurones carrying Ca^{2+}-permeable AMPA receptors in the visual cortex are GABAergic (Jonas *et al.* 1994). It is likely that Ca^{2+}-permeable AMPA receptors are dominantly expressed in GABAergic interneurones. As the next step, it is important to identify the neurones receiving axonal projections from type II or intermediate neurones and to record post-synaptic events from those neurones elicited by stimulating type II or intermediate neurones.

The present study has shown that inwardly rectifying and Ca^{2+}-permeable AMPA receptors are involved in the excitatory synaptic transmission in type II neurones. Type II neurones carry NMDA receptors, which are highly permeable to Ca^{2+} (MacDermott *et al.* 1986; Mayer & Westbrook, 1987), and these NMDA receptors are also involved in the synaptic transmission in type II neurones. It is now widely accepted that NMDA receptors participate in causing plastic changes of synaptic functions by regulating intracellular Ca^{2+} concentrations (Bliss & Collingridge, 1993). NMDA receptors are permeable to Ca^{2+} at depolarized membrane potentials, whereas type II AMPA receptors allow Ca^{2+} to permeate at more hyperpolarized levels, near the resting membrane potential. Although the specific role of type II AMPA receptors is presently unknown, these two types of Ca^{2+}-permeable receptors might play different functional roles by regulating Ca^{2+} entry in different contexts. Some polyamine-containing arthropod toxins such as joro-spider toxin and philantotoxin-433 have been shown to be specific antagonists of type II AMPA receptors (Blaschke, Keller, Rivosecchi, Hollmann, Heinemann & Konnerth, 1993; Washburn & Dingledine, 1994). Such specific antagonists could be useful tools for investigating the functional significance of type II AMPA receptors in the neural circuits of both the hippocampus and the neocortex.

Blaschke, M., Keller, B. U., Rivosecchi, R., Hollmann, M., Heinemann, S. & Konnerth, A. (1993). A single amino acid determines the subunit-specific spider toxin block of α-amino-3-hydroxy-5-methylisoxazole-4-propionate/kainate receptor channels. *Proceedings of the National Academy Sciences of the USA* **90**, 6528–6532.

Bliss, T. V. P. & Collingridge, G. L. (1993). A synaptic model of memory: long-term potentiation in the hippocampus. *Nature* **361**, 31–39.

Bochet, P., Audinat, E., Lambolez, B., Crépel, F., Rossier, J., Iino, M., Tsuzuki, K. & Ozawa, S. (1994). Subunit composition at the single-cell level explains functional properties of a glutamate-gated channel. *Neuron* **12**, 383–388.

Bowie, D. & Mayer, M. L. (1995). Inward rectification of both AMPA and kainate subtype glutamate receptors generated by polyamine-mediated ion channel block. *Neuron* **15**, 453–462.

Burnashev, N., Khodorova, A., Jonas, P., Helm, P. J., Wisden, W., Monyer, H., Seeburg, P. H. & Sakmann, B. (1992). Calcium-permeable AMPA-kainate receptors in fusiform cerebellar glial cells. *Science* **256**, 1566–1570.

Donevan, S. D. & Rogawski, M. A. (1995). Intracellular polyamines mediate inward rectification of Ca^{2+}-permeable AMPA receptors. *Proceedings of the National Academy Sciences of the USA* **92**, 9298–9302.

Edwards, F. A., Konnerth, A., Sakmann, B. & Takahashi, T. (1989). A thin slice preparation for patch clamp recordings from neurones of the mammalian central nervous system. *Pflügers Archiv* **414**, 600–612.

Egebjerg, J., Bettler, B., Hermans-Borgmeyer, I. & Heinemann, S. (1991). Cloning of a cDNA for a glutamate receptor subunit activated by kainate but not AMPA. *Nature* **351**, 745–748.

Geiger, J. R. P., Melcher, T., Koh, D.-S., Sakmann, B., Seeburg, P. H., Jonas, P. & Monyer, H. (1995). Relative abundance of subunit mRNAs determines gating and Ca^{2+} permeability of AMPA receptors in principal neurons and interneurons in rat CNS. *Neuron* **15**, 193–204.

Gilbertson, T. A., Scobey, R. & Wilson, M. (1991). Permeation of calcium ions through non-NMDA glutamate channels in retinal bipolar cells. *Science* **251**, 1613–1615.

Hollmann, M. & Heinemann, S. (1994). Cloned glutamate receptors. *Annual Review of Neuroscience* **17**, 31–108.

Horikawa, K. & Armstrong, W. E. (1988). A versatile means of intracellular labeling: injection of biocytin and its detection with avidin conjugates. *Journal of Neuroscience Methods* **25**, 1–11.

Iino, M., Mochizuki, S. & Ozawa, S. (1994). Relationshipship between calcium permeability and rectification properties of AMPA receptors in cultured rat hippocampal neurons. *Neuroscience Letters* **173**, 14–16.

Iino, M., Ozawa, S. & Tsuzuki, K. (1990). Permeation of calcium through excitatory amino acid receptor channels in cultured rat hippocampal neurones. *Journal of Physiology* **424**, 151–165.

Isa, T., Iino, M., Itazawa, S. & Ozawa, S. (1995). Spermine mediates inward rectification of calcium-permeable AMPA receptor channels. *NeuroReport* **6**, 2045–2048.

Jonas, P., Racca, C., Sakmann, B., Seeburg, P. H. & Monyer, H. (1994). Differences in Ca^{2+} permeability of AMPA-type glutamate receptor channels in neocortical neurons caused by differential GluR-B subunit expression. *Neuron* **12**, 1281–1289.

Jonas, P. & Sakmann, B. (1992). Glutamate receptor channels in isolated patches from CA1 and CA3 pyramidal cells of rat hippocampal slices. *Journal of Physiology* **455**, 143–171.

Kamboj, S. K., Swanson, G. T. & Cull-Candy, S. G. (1995). Intracellular spermine confers rectification on rat calcium-permeable AMPA and kainate receptors. *Journal of Physiology* **486**, 297–303.

Keinänen, K., Wisden, W., Sommer, B., Werner, P., Herb, A., Verdoorn, T. A., Sakmann, B. & Seeburg, P. H. (1990). A family of AMPA-selective glutamate receptors. *Science* **249**, 556–560.

Keller, B. U., Konnerth, A. & Yaari, Y. (1991). Patch clamp analysis of excitatory synaptic currents in granule cells of rat hippocampus. *Journal of Physiology* **435**, 275–293.

Koh, D.-S., Burnashev, N. & Jonas, P. (1995). Block of native Ca^{2+}-permeable AMPA receptors in rat brain by intracellular polyamines generates double rectification. *Journal of Physiology* **486**, 305–312.

Koh, D.-S., Geiger, J. R. P., Jonas, P. & Sakmann, B. (1995). Ca^{2+}-permeable AMPA and NMDA receptor channels in basket cells of rat hippocampal dentate gyrus. *Journal of Physiology* **485**, 383–402.

Lerma, J., Morales, M., Ibarz, J. M. & Somohano, F. (1994). Rectification properties and Ca^{2+} permeability of glutamate receptor channels in hippocampal cells. *European Journal of Neuroscience* **6**, 1080–1088.

Lerma, J., Paternain, A. V., Naranjo, J. R. & Mellström, B. (1993). Functional kainate-selective glutamate receptors in cultured hippocampal neurons. *Proceedings of the National Academy Sciences of the USA* **90**, 11688–11692.

McBain, C. J. & Dingledine, R. (1993). Heterogeneity of synaptic glutamate receptors on CA3 stratum radiatum interneurones of rat hippocampus. *Journal of Physiology* **462**, 373–392.

MacDermott, A. B., Mayer, M. L., Westbrook, G. L., Smith, S. J. & Barker, J. L. (1986). NMDA-receptor activation increases cytoplasmic calcium concentration in cultured spinal cord neurones. *Nature* **321**, 519–522.

Mayer, M. L. & Westbrook, G. L. (1987). Permeation and block of *N*-methyl-D-aspartic acid receptor channels by divalent cations in mouse cultured central neurones. *Journal of Physiology* **394**, 501–527.

Monyer, H., Seeburg, P. H. & Wisden, W. (1991). Glutamate-operated channels: Developmentally early and mature forms arise by alternative splicing. *Neuron* **6**, 799–810.

Müller, T., Möller, T., Berger, T., Schnitzer, J. & Kettenmann, H. (1992). Calcium entry through kainate receptors and resulting potassium-channel blockade in Bergmann glial cells. *Science* **256**, 1563–1566.

Nicoll, R. A., Malenka, R. C. & Kauer, J. A. (1990). Functional comparison of neurotransmitter receptor subtypes in mammalian central nervous system. *Physiological Reviews* **70**, 513–565.

Ozawa, S. & Iino, M. (1993). Two distinct types of AMPA responses in cultured rat hippocampal neurons. *Neuroscience Letters* **155**, 187–190.

Ozawa, S., Iino, M. & Abe, M. (1991*a*). Excitatory synapse in the rat hippocampus in tissue culture and effects of aniracetam. *Neuroscience Research* **12**, 72–82.

Ozawa, S., Iino, M. & Tsuzuki, K. (1991*b*). Two types of kainate response in cultured rat hippocampal neurons. *Journal of Neurophysiology* **66**, 2–11.

Partin, K. M., Patneau, D. K. & Mayer, M. L. (1994). Cyclothiazide differentially modulates desensitization of α-amino-3-hydroxy-5-methyl-4-isoxazole propionic acid receptor splice variants. *Molecular Pharmacology* **46**, 129–138.

Partin, K. M., Patneau, D. K., Winters, C. A., Mayer, M. L. & Buonanno, A. (1993). Selective modulation of desensitization at AMPA *versus* kainate receptors by cyclothiazide and concanavalin A. *Neuron* **11**, 1069–1082.

Sather, W., Dieudonné, S., MacDonald, J. F. & Ascher, P. (1992). Activation and desensitization of *N*-methyl-D-aspartate receptors in nucleated outside-out patches from mouse neurones. *Journal of Physiology* **450**, 643–672.

Seeburg, P. H. (1993). The molecular biology of mammalian glutamate receptor channels. *Trends in Neurosciences* **16**, 359–365.

Sommer, B., Keinänen, K., Verdoorn, T. A., Wisden, W., Burnashev, N., Herb, A., Köhler, M., Takagi, T., Sakmann, B. & Seeburg, P. H. (1990). Flip and flop: A cell-specific functional switch in glutamate-operated channels of the CNS. *Science* **249**, 1580–1585.

SPRUSTON, N., JONAS, P. & SAKMANN, B. (1995). Dendritic glutamate receptor channels in rat hippocampal CA3 and CA1 pyramidal neurons. *Journal of Physiology* **482**, 325–352.

WASHBURN, M. S. & DINGLEDINE, R. (1994). Selective blockade of calcium-permeable AMPA receptors by spermine and polyamine arthropod toxins. *Abstracts of Society for Neuroscience* **310**, 4.

Acknowledgements

This investigation was supported by grants from the Human Frontier Science Program and the Ministry of Education, Science and Culture of Japan.

Received 30 January 1995; accepted 2 October 1995.